Mechanical Technology and Engineering Insights

www.mtei.reapress.com

Mech. Technol. Eng. Insights. Vol. 3, No. 3 (2026) 205–215.

Paper Type: Original Article

Nonlinear Optimal Control of Spacecraft Attitude with Reduced-Order Observer-Based State Estimation

Mohammadreza Kazempoor[1,*], Mojtaba Malekee[2]

[1] Department of Mechanical Engineering, Lahijan Brunch, Islamic Azad University, Lahijan, Iran; m.kazempour1981@iau.ac.ir.
[2] Department of Mechanical Engineering, Faculty of Mechanical Engineering, University of Guilan, Rasht, Guilan, Iran; mojtaba.malekee@gmail.com.

Citation:

Received: 12 April 2026 *Revised: 27 June 2026* *Accepted: 12 August 2026*	Kazempoor, M., & Malekee, M. (2026). Nonlinear optimal control of spacecraft attitude with reduced-order observer-based state estimation. *Mechanical Technology and Engineering Insights, 3*(3), 205-215.

Abstract

This paper addresses the nonlinear attitude-tracking control problem of a rigid spacecraft with large-angle manoeuvres under actuator saturation and partial state measurement. A combined control and state-estimation framework is developed by combining feedback linearisation, Linear Quadratic Regulation (LQR), and a reduced-order Luenberger observer. First, the feedback linearisation is used to transform the nonlinear attitude dynamics into a linear equivalent form, which allows the LQR controller to be designed systematically to balance the attitude-tracking performance and control effort. The developed control architecture is implemented subject to actuator torque constraints to reflect the practical limitations encountered during large-angle manoeuvres. A reduced-order observer is added to the system to estimate the required unmeasured states from the available measurements and the system dynamics, reducing dependence on direct attitude measurements. The proposed framework is validated with numerical simulations using the TURKSAT-1B spacecraft parameters. The simulation results are used to evaluate the attitude-tracking accuracy, transient response, control effort, actuator saturation, and observer convergence. The results demonstrate the potential of combining nonlinear feedback linearisation and optimal linear control with reduced-order state estimation to achieve satisfactory attitude tracking under the given operating conditions. The paper proposes a computationally structured approach to spacecraft attitude control when not all required states can be measured directly.

Keywords: Spacecraft attitude control, Nonlinear feedback linearisation, Linear quadratic regulator, Reduced order observer, Luenberger observer, Actuator saturation, State estimation.

1 | Introduction

Attitude control of spacecraft is a fundamental part of guidance, navigation, and control systems, directly affecting pointing accuracy, communication performance, and mission effectiveness. Large-angle attitude

Corresponding Author: m.kazempour1981@iau.ac.ir
https://doi.org/10.48313/mtei.v3i3.89
Licensee System Analytics. This article is an open access article distributed under the terms and conditions of the Creative Commons Attribution (CC BY) license (http://creativecommons.org/licenses/by/4.0).

manoeuvres pose a serious control challenge because of the nonlinear nature of spacecraft rotational dynamics and attitude kinematics [1–4].

Therefore, developing control strategies with accurate tracking, acceptable control effort, and satisfactory performance under practical constraints remains an important research topic. Several mathematical representations describe spacecraft orientation, such as Euler angles, rotation matrices, unit quaternions, and modified Rodrigues parameters [1], [2]. Euler angles are intuitive, but their kinematic equations can have singularities. For large angle manoeuvres, unit quaternions are commonly used to avoid these singularities. However, the unit-norm constraint has to be maintained [3], [4]. Linear control techniques, especially the Linear Quadratic Regulator (LQR), offer systematic ways to design feedback controllers by minimising a quadratic performance index which includes state errors and control effort. LQR-based methods have been explored for spacecraft attitude tracking and optimal manoeuvring, with applications involving flexible spacecraft and online system identification [5–7].

However, controllers based on linearised models may degrade when the spacecraft operates far from the nominal equilibrium or performs large-angle manoeuvres. Feedback linearisation is a well-known nonlinear control technique that uses a state-dependent control transformation to compensate for modelled nonlinearities, so that linear control techniques can be applied to the resulting dynamics under suitable conditions [8], [9]. Singh and Yim [10] considered feedback linearisation for satellite attitude control using solar-radiation-pressure-generated torque. Bang et al. [11] considered feedback-linearization-based attitude control for rigid spacecraft. Nonlinear spacecraft manoeuvring and prescribed attitude-error dynamics have been further studied in [12].

Thus, combining feedback linearisation with LQR provides a potentially efficient framework that unifies nonlinear compensation with a systematic approach to optimal control design. However, its performance depends on model accuracy and the validity of the feedback transformation.Another major challenge is the availability of the state variables required for the feedback control. Spacecraft use gyroscopes to measure angular velocities, and attitude sensors like star trackers and Sun sensors provide orientation information [2]. Gyroscope measurements are subject to noise, bias, and drift, so integrating angular velocities alone does not generally give a permanently accurate estimate of absolute attitude.

Hence, reliable state estimation must consider measurement availability, initial conditions, and system observability. State observers use available measurements and a mathematical model to reconstruct unmeasured variables. For linear systems, the classical approach is the Luenberger observer, where convergence depends on the system's observability properties and the choice of observer gain [15]. If the remaining states are available from measurements, a reduced-order observer estimates only the unmeasured states, reducing computational requirements.

Crassidis and Markley [13] studied unscented filtering for attitude estimation for spacecraft applications using gyroscopic propagation and attitude measurements, and Crassidis et al. [14] reviewed nonlinear attitude estimation techniques and their applications. These studies emphasise the importance of sensor modelling, estimation accuracy, and having enough information for attitude reconstruction.

In addition, actuator saturation is a practical limitation, since the controller may request torque beyond the actuator's physical capacity. Such limitations may increase tracking errors, slow down transient response, and impair closed-loop stability. Bang et al. [16] studied large-angle attitude control with actuator saturation.

Lu et al. [17] studied spacecraft attitude tracking with saturation, inertia uncertainties, and external disturbances. Actuator faults and constrained control inputs have also been investigated by adaptive and sliding-mode approaches [18]. These results highlight the need to test spacecraft controllers under realistic actuator constraints.Other approaches have developed methods to improve robustness to uncertainty and disturbances. For flexible spacecraft attitude manoeuvring under external disturbances, inertia uncertainty, and input constraints, Bai et al. [19] proposed robust nonlinear (H_\infty) output-feedback control.

Moreover, large-angle manoeuvres with guaranteed-cost control based on sum-of-squares optimisation and linear parameter-varying representations have been considered [20]. Further studies have been carried out on rigid-body attitude control, adaptive manoeuvring and robust control of flexible spacecraft [21–23]. Further, nonlinear attitude recovery and stability were studied by Tafazoli and Khorasani [24]. Kothari et al. [25] developed a unified anti-windup framework to address the effects of actuator constraints in feedback systems. Although these methods offer valuable advantages, their implementation may require greater computational resources or more sophisticated controller-design procedures.Despite these advances, nonlinear dynamics, incomplete state measurements, and actuator saturation still significantly affect spacecraft attitude tracking. More specifically, observer estimation errors can affect the performance of a controller designed using the full state vector, and actuator saturation can cause the actual control input to differ from the desired control command.

Hence, this paper examines a nonlinear spacecraft attitude-control scheme based on feedback linearisation and LQR with a reduced-order Luenberger observer. The simulation model considers actuator torque saturation. The proposed approach is validated using TURKSAT-1B spacecraft parameters. The main contributions are: 1) the combination of feedback linearisation with LQR for large-angle attitude tracking, 2) the introduction of reduced-order state estimation under given measurement and observability conditions; and, 3) the evaluation of tracking performance, control effort, observer behaviour, and actuator saturation by numerical simulations.

2|Nonlinear Spacecraft Dynamic Equations

This section briefly reviews the kinematic and dynamic equations of motion for a three-axis-stabilized spacecraft.

The attitude dynamic equations are obtained from Euler's moment equations as follows:

$$\tau = \dot{h}_I = \dot{h}_B + \omega \times h. \tag{1}$$

In this equation, the subscript "I" indicates a derivative in the inertial frame, while the subscript "B" indicates a derivative in the rotating body frame. Hence, the attitude dynamics in principal axes can be written as:

$$\begin{aligned} I_x\dot{\omega}_x + (I_z - I_y)\omega_y\omega_z &= \tau_x, \\ I_y\dot{\omega}_y + (I_x - I_z)\omega_z\omega_x &= \tau_y, \\ I_z\dot{\omega}_z + (I_y - I_x)\omega_x\omega_y &= \tau_z, \end{aligned} \tag{2}$$

Where $U = [u_1 \quad u_2 \quad u_3]^T = [\tau_x \quad \tau_y \quad \tau_z]^T$are the control torques acting on the satellite $I_x I_y$, and I_z are the principal moments of inertia.

The Euler parameter θ used for attitude representation of the body-fixed frame with respect to an inertial frame is given by:

$$\dot{\theta} = R\omega, \tag{3}$$

$$R^{-1} = \begin{bmatrix} 1 & 0 & -\sin\theta_2 \\ 0 & \cos\theta_1 & \sin\theta_1\cos\theta_2 \\ 0 & -\sin\theta_1 & \cos\theta_1\cos\theta_2 \end{bmatrix}. \tag{4}$$

For small Euler angles, the angular velocities of the body frame are described by the following equation:

$$\begin{aligned} \omega_x &\approx \dot{\phi} - \omega_0\psi, \\ \omega_y &\approx \dot{\theta} - \omega_0, \\ \omega_z &\approx \dot{\psi} + \omega_0\phi. \end{aligned} \tag{5}$$

Therefore, the nonlinear equations of motion for spacecraft can be written as:

$$\begin{cases} \ddot{\phi} = f_1(X) + g_1(X)u_1, \\ \ddot{\theta} = f_2(X) + g_2(X)u_2, \\ \ddot{\psi} = f_3(X) + g_3(X)u_3, \end{cases} \quad (6)$$

where:

$$\begin{cases} f_1(X) = \omega_0\dot{\psi} - \dfrac{(I_z - I_y)\omega_y\omega_z}{I_x}, \\ f_2(X) = -\dfrac{(I_x - I_z)\omega_z\omega_x}{I_y}, \\ f_3(X) = -\omega_0\dot{\phi} - \dfrac{(I_y - I_x)\omega_x\omega_y}{I_z}. \end{cases} \quad (7)$$

And

$$\begin{cases} g_1(X) = \dfrac{1}{I_x}, \\ g_2(X) = \dfrac{1}{I_y}, \\ g_3(X) = \dfrac{1}{I_z}, \end{cases} \quad (8)$$

$$X = [\phi \quad \theta \quad \psi \quad \dot{\phi} \quad \dot{\theta} \quad \dot{\psi}]^T. \quad (9)$$

3 | Nonlinear Control Design Using the Feedback Linearization Method

The feedback linearization technique is based on a linearized input-output relationship. It consists of two controller loops: An inner loop (nonlinear controller) to eliminate nonlinear terms in the model dynamics and an outer loop (linear controller) to control the linearized model (see *Fig. 1*).

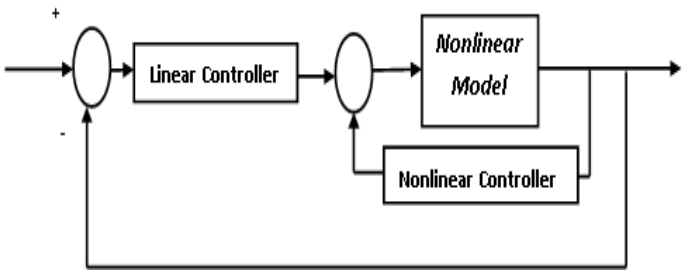


Fig. 1. Feedback linearization method.

By considering the spacecraft dynamic equations *Eqs. (6)-(8)*, also by assuming the output Y such as:

$$y = \begin{bmatrix} y_1 \\ y_2 \\ y_3 \end{bmatrix} = \begin{bmatrix} \phi \\ \theta \\ \psi \end{bmatrix}. \quad (10)$$

The successive differentiation process is done on the output (attitude angle) until the control signal appears:

$$\ddot{y} = \begin{bmatrix} \ddot{\phi} \\ \ddot{\theta} \\ \ddot{\psi} \end{bmatrix} = [f(X)] + [g(X)]\ [u]. \quad (11)$$

$$\ddot{y}_i = \nu_i, \qquad i = 1,2,3. \tag{12}$$

The control law can be obtained from the following equation:

$$[u_i] = [\nu_i - f_i][g_i]^{-1}, \qquad i = 1,2,3. \tag{13}$$

Considering saturation, we choose a larger control-weight matrix, as shown in *Fig. 2* [1].

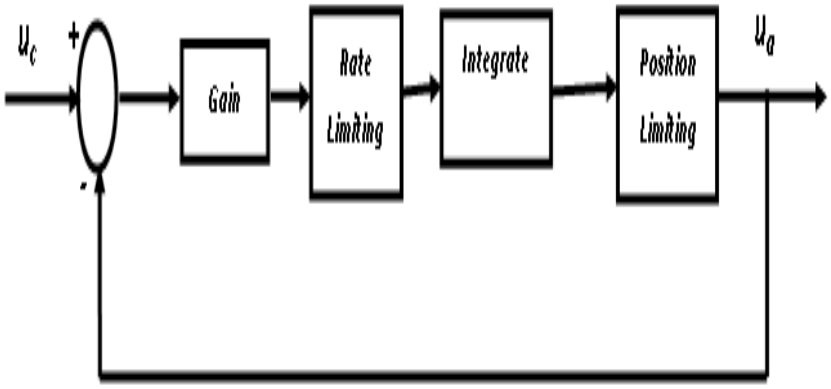


Fig. 2. Enforcing control saturation limits.

3.1 | Linear Controller LQR Design

In the optimal control problem, it is desirable to obtain the state feedback gain matrix K, such that the quadratic integral criterion (J) is minimized. Quadratic integral criterion:

$$J = \int_0^\infty [X^T Q X + U^T R U] dt. \tag{14}$$

Q and R are weighting matrices that penalize certain states and control inputs. Q is positive semi-definite, while R is positive definite. If the system is disturbed and offset from the zero state, the control ν (equivalent input) can bring the system back to the zero state while minimizing J [9]. The solution to this problem is the feedback law as shown:

$$U_{(t)} = -R^{-1} B^T P_{(t)} X_{(t)}, \tag{15}$$

where P(t) is the solution of the Riccati equation:

$$A^T P + PA - PBR^{-1} B^T P + Q = 0. \tag{16}$$

The linear optimal feedback matrix can be obtained:

$$K = R^{-1} B^T P. \tag{17}$$

The Riccati equation can be solved numerically for given A, B, R, and Q. By varying the weights of Q and R and selecting the best result, K can be optimized.

Notice: The A, B, C, Q, and R matrices are not the same matrices that are considered for conventional linearization (i.e., Jacobian linearization).

3.2 | Reduced-Order Observer Design

Consider the following Multi-Input Multi-Output (MIMO) system that is linearized around the equilibrium point:

$$\begin{cases} \dot{X}_{n\times 1} = A_{n\times n}X_{n\times 1} + B_{n\times m}U_{m\times 1} \\ Y_{l\times 1} = C_{l\times n}X_{n\times 1}. \end{cases} \quad (18)$$

Where: n: dimension of $X_{(t)}$, m: dimension of $U_{(t)}$, l: dimension of $Y_{(t)}$ The dynamics of the reduced-order Luenberger observer with state vector $Z_{(t)}$ is defined by:

$$\dot{Z}_{(t)} = DZ_{(t)} + TY_{(t)} + RU_{(t)}. \quad (19)$$

According to *Fig. 3*, the reduced-order observer design depends on the choice of the R, T, and D matrices.

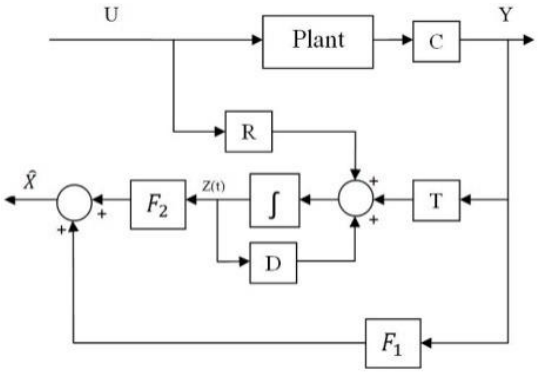


Fig. 3. Observer block diagram.

3.2.1 | Steps of design

Choose matrix D by determining the n-l eigenvalues of the observer. The eigenvalues of matrix D specify the rate at which the estimation error decays to zero. By changing this matrix, the rate of estimation is changed. The transformation matrix margin Q can be obtained from the following equation:

$$CQ = [0_{l\times n-l} \quad I_l]. \quad (20)$$

Moreover, multiplying LQ can be broken as follows:

$$LQ = [I_{n-l} \quad \tilde{L}_{n-l\times l}]. \quad (21)$$

Also, the matrix A can be resolved with the transformation matrix Q, as the following equation:

$$\tilde{A} = Q^{-1}AQ = \begin{bmatrix} \tilde{A}_{11} & \tilde{A}_{12} \\ \tilde{A}_{21} & \tilde{A}_{22} \end{bmatrix} \quad (22)$$

By using the following equations, $\tilde{L}$ and T can be obtained:

$$\tilde{A}_{11} + \tilde{L}\tilde{A}_{21} = D. \quad (23)$$

$$\tilde{A}_{12} + \tilde{L}\tilde{A}_{22} - D\tilde{L} = T. \quad (24)$$

Then, the matrices L and R are defined:

$$L = [I_{n-l} \quad \tilde{L}_{n-l\times l}]Q^{-1}. \tag{25}$$

$$R = LB. \tag{26}$$

Finally, the matrices $F_1F_2$and $\hat{X}$ are obtained as:

$$\begin{bmatrix} C \\ L \end{bmatrix}^{-1} = [F_1 \quad F_2]. \tag{27}$$

$$\hat{X} = F_1Y + F_2Z. \tag{28}$$

The observer design relies on transforming the system into a suitable coordinate representation that separates the measured and unmeasured states. The transformed matrices are then partitioned according to these two sets of states. In this representation, the reduced-order observer gain is chosen such that the eigenvalues of the estimation-error dynamics lie in the desired stable region of the complex plane.

The design has the following major steps:

I. Observer dynamics selection. Choose desired eigenvalues for the reduced-order estimation-error system. These eigenvalues determine the estimation-error convergence rate. They should be chosen to provide sufficiently fast estimation without too much sensitivity to measurement noise or model uncertainty.

II. A coordinate transformation is created. Find a nonsingular transformation matrix separating measured states from unmeasured states. Transform the system matrices. The corresponding partition representation is.

III. Determine the observer gain. Calculate the reduced-order observer gain using the transformed system matrices and the desired observer poles. The gain should be chosen so that the estimation-error dynamics are asymptotically stable.

IV. Observer matrix reconstruction. The matrices required to represent the observer in the original state coordinates are calculated, and the derived estimation equations are implemented by means of the available measurements and control inputs.

V. Assess the estimation performance. Verify convergence of the estimation error for the given initial conditions and system parameters. Also, the observer should be evaluated in the presence of measurement noise, parameter uncertainty, and actuator saturation where applicable.

The structure of the reduced-order observer is shown in *Fig. 3*. Implementation requires clear separation of measured and unmeasured states and observability analysis of the system. The specific transformation and gain equations can be derived using the spacecraft model's real matrices.

4 | Simulation Results and Discussion

To assess the performance of the proposed nonlinear feedback linearisation controller combined with the LQR method and reduced-order observer, numerical simulations are conducted. Gyroscopes measure the spacecraft's angular velocities, and the observer estimates the Euler angles. The reference spacecraft is chosen as the satellite TURKSAT-1B [8], and the moment of inertia matrix is given by

$$I = \mathrm{diag}(3770,730,4020)\ \mathrm{kg,m^2}.$$

The initial attitude and angular velocities are specified according to the simulation conditions, while the desired Euler angles are set to

$$\begin{bmatrix} \phi_{in} \\ \theta_{in} \\ \psi_{in} \end{bmatrix} = \begin{bmatrix} 3 \\ 4 \\ 5 \end{bmatrix} \quad \mathrm{Deg}.$$

$$\begin{bmatrix}\omega_{ix}\\ \omega_{iy}\\ \omega_{iz}\end{bmatrix} = \begin{bmatrix}0\\ 0\\ 0\end{bmatrix} \text{ Rad/sec.}$$

$$\begin{bmatrix}\phi_f\\ \theta_f\\ \psi_f\end{bmatrix} = \begin{bmatrix}10\\ 20\\ 30\end{bmatrix} \text{ Deg.}$$

Fig. 4 compares the actual and estimated Euler angles with their respective reference values. All attitude components move toward their desired values, indicating good tracking performance during the large-angle manoeuvre. The estimated roll and yaw angles show moderate transient overshoots, whereas the pitch angle responds faster with relatively small estimation error. The differences between the real and estimated attitudes decrease gradually, showing convergence of the observer estimates.

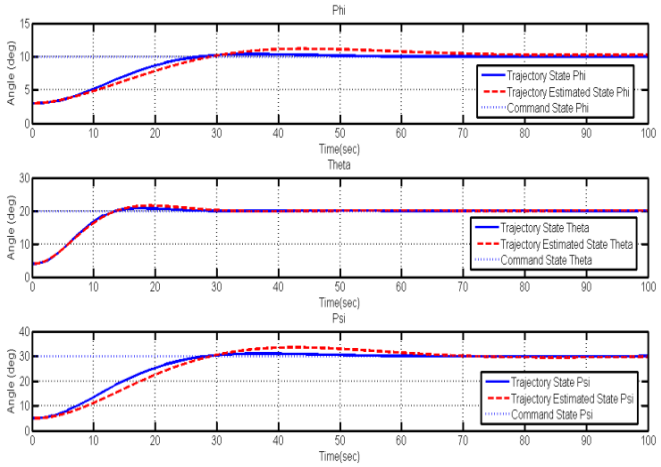


Fig. 4. Real and estimated spacecraft attitude.

Fig. 5 shows the angular velocity responses for the spacecraft's three axes. The angular velocities decrease to zero with a damped transient behaviour after an initial increase during the manoeuvre. This demonstrates the proposed controller's effectiveness in attenuating rotational motion as the spacecraft approaches the target orientation.

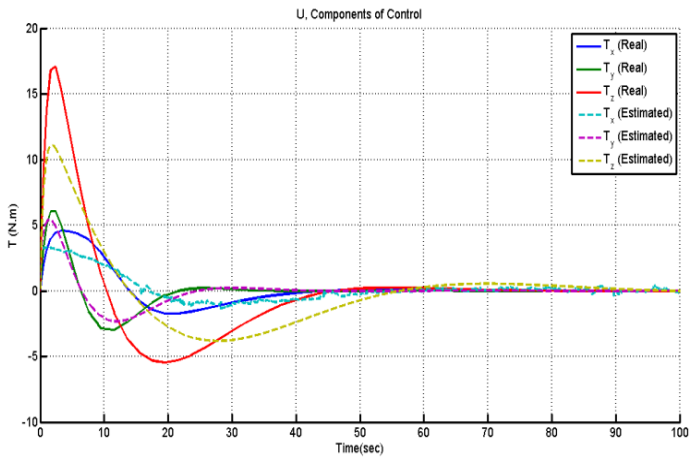


Fig. 5. Angular velocity of spacecraft.

The control torque components with real states and observer-estimated states are shown in *Fig. 6*. The biggest transient torque is along the third axis, and it is about 17 N·m. In contrast, the other components are smaller. The differences between the two control strategies are significant in the first transient, but the torque responses tend to zero as the system is stabilised.

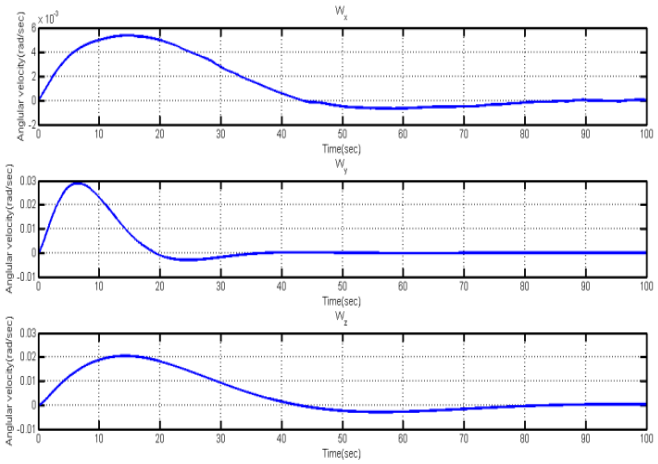


Fig. 6. Control input signals.

The simulation results verify the effectiveness of the proposed control strategy for attitude tracking and observer-based state estimation. Combining feedback linearization with the LQR approach provides satisfactory transient performance, and the reduced-order observer reconstructs the unmeasured attitude states from the available measurements. The satisfaction of actuator saturation constraints should be checked in accordance with the specified torque limits.

5 | Conclusion

This paper investigates a nonlinear spacecraft attitude control strategy based on feedback linearisation, LQR, and a reduced-order Luenberger observer. We performed numerical simulations using the dynamic parameters of the TURKSAT-1B spacecraft to test the proposed framework. According to the results obtained, we can make the following conclusions:

I. The combined feedback linearisation and LQR controller achieved satisfactory attitude tracking during the simulated large-angle manoeuvre, with all three Euler angles tending toward their stated reference values.

II. The reduced-order observer could reconstruct the unmeasured attitude states from the available angular velocity measurements. The differences between the actual and estimated attitudes decreased over time, showing convergence of the estimated states.

III. The angular velocities showed damped transient responses and gradually approached zero, indicating that the rotational motion was effectively suppressed when the spacecraft reached the desired orientation.

IV. Following the initial transient, the control torques reduced to zero, with the maximum reported torque being approximately 17 N·m about the third axis. The differences between the control inputs calculated from the actual and estimated states decreased as the system settled down.

The overall results demonstrate the promise of integrating nonlinear feedback linearisation, optimal control, and reduced-order state estimation for spacecraft attitude tracking under partial state measurements. However, further investigations are needed to quantify performance under actuator saturation, measurement noise, external disturbances, and model uncertainties, and to establish robustness under more realistic operating conditions.

Conflict of Interest

The authors declare that they have no competing interests.

Data Availability

The data supporting the findings of this study are available within the article.

Funding

This research did not receive any external funding.

References

[1] Shuster, M. D. (1993). A survey of attitude representations. *Navigation*, *8*(9), 439-517. https://www.malcolmdshuster.com/Pub_1993h_J_Repsurv_scan.pdf

[2] Forbes, J. R. (2015). Fundamentals of spacecraft attitude determination and control [bookshelf]. *IEEE Control Systems Magazine*, *35*(4), 56-58. https://doi.org/10.1007/978-1-4939-0802-8.

[3] Wie, B., & Barba, P. M. (1985). Quaternion feedback for spacecraft large angle maneuvers. *Journal of guidance, Control, and Dynamics*, *8*(3), 360-365. https://doi.org/10.2514/3.19988.

[4] Wen, J. T. Y., & Kreutz-Delgado, K. (1991). The attitude control problem. *IEEE transactions on automatic control*, *36*(10), 1148-1162. https://doi.org/10.2514/3.19988

[5] Moradi, M., Menhaj, M. B., & Ghasemi, A. (2012). Attitude tracking control using an online identification and a linear quadratic regulator–based strategy in the presence of orbital eccentricity. *Journal of Aerospace Engineering*, *25*(1), 71-79. https://doi.org/10.1061/(ASCE)AS.1943-5525.0000098

[6] Zheng, J., Banks, S. P., & Alleyne, H. (2005). Optimal attitude control for three-axis stabilized flexible spacecraft. *Acta astronautica*, *56*(5), 519-528. https://doi.org/10.1016/j.actaastro.2004.10.002

[7] Guarnaccia, L., Bevilacqua, R., & Pastorelli, S. P. (2016). Suboptimal LQR-based spacecraft full motion control: Theory and experimentation. *Acta Astronautica*, *122*, 114-136. https://doi.org/10.1016/j.actaastro.2016.01.016

[8] Isidori, A. (1995). *Nonlinear control systems*. London: Springer. https://doi.org/10.1007/978-1-84628-615-5

[9] Khalil, H. K., & Grizzle, J. W. (2002). *Nonlinear systems* (Vol. 3, p. 126). Upper Saddle River, NJ: Prentice hall. https://files.dooctly.com/samples/solution-manual-nonlinear-systems-3e-khalil.pdf

[10] Singh, S. N., & Yim, W. (1996). Feedback linearization and solar pressure satellite attitude control. *IEEE transactions on aerospace and electronic systems*, *32*(2), 732-741. https://doi.org/10.1109/7.489516

[11] Bang, H., Lee, J. S., & Eun, Y. J. (2004). Nonlinear attitude control for a rigid spacecraft by feedback linearization. *KSME international journal*, *18*(2), 203-210. https://doi.org/10.1007/BF03184729.

[12] Bajodah, A. H. (2008). Singularly perturbed feedback linearization with linear attitude deviation dynamics realization. *Nonlinear Dynamics*, *53*(4), 321-343. https://doi.org/10.1007/s11071-007-9316-0

[13] Crassidis, J. L., & Markley, F. L. (2003). Unscented filtering for spacecraft attitude estimation. *Journal of guidance, control, and dynamics*, *26*(4), 536-542. https://doi.org/10.2514/2.5102.

[14] Crassidis, J. L., Markley, F. L., & Cheng, Y. (2007). Survey of nonlinear attitude estimation methods. *Journal of guidance, control, and dynamics*, *30*(1), 12-28. https://doi.org/10.2514/1.22452.

[15] Luenberger, D. G. (1964). Observing the state of a linear system. *IEEE transactions on military electronics*, *8*(2), 74-80. https://doi.org/10.1109/TME.1964.4323124.

[16] Bang, H., Tahk, M. J., & Choi, H. D. (2003). Large angle attitude control of spacecraft with actuator saturation. *Control engineering practice*, *11*(9), 989-997. https://doi.org/10.1016/S0967-0661(02)00216-2

[17] Lu, K., Xia, Y., & Fu, M. (2013). Controller design for rigid spacecraft attitude tracking with actuator saturation. *Information sciences*, *220*, 343-366. https://doi.org/10.1016/j.ins.2012.07.039

[18] Han, Z., Wang, M., Yan, X., & Qian, H. (2021). Adaptive fixed-time nonsingular terminal sliding mode attitude tracking control for spacecraft with actuator saturations and faults. *International journal of aerospace engineering*, *2021*(1), 8838784. https://doi.org/10.1155/2021/8838784

[19] Bai, H., Huang, C., & Zeng, J. (2019). Robust nonlinear H∞ output-feedback control for flexible spacecraft attitude manoeuvring. *Transactions of the institute of measurement and control*, *41*(7), 2026-2038. https://doi.org/10.1177/0142331218794378.

[20] Qingliang, M., Haiyan, Y., Ruihua, Y., & Xiangyu, C. (2012, July). Optimal guaranteed cost control of spacecraft large angle attitude maneuvers. *Proceedings of the 31st Chinese control conference* (pp. 2307-2311). IEEE. https://ieeexplore.ieee.org/abstract/document/6390309

[21] Chaturvedi, N. A., Sanyal, A. K., & McClamroch, N. H. (2011). Rigid-body attitude control. *IEEE control systems magazine*, *31*(3), 30-51. https://doi.org/10.1109/MCS.2011.940459.

[22] Parlos, A. G., & Sunkel, J. W. (1992). Adaptive attitude control and momentum management for large-angle spacecraft maneuvers. *Journal of guidance, control, and dynamics*, *15*(4), 1018-1028. https://doi.org/10.2514/3.20937

[23] Singh, S. N. (1987). Robust nonlinear attitude control of flexible spacecraft. *IEEE transactions on aerospace and electronic systems*, *23*(3), 380-387. https://doi.org/10.1109/TAES.1987.310836

[24] Tafazoli, S., & Khorasani, K. (2006). Nonlinear control and stability analysis of spacecraft attitude recovery. *IEEE transactions on aerospace and electronic systems*, *42*(3), 825-845. https://doi.org/10.1109/TAES.2006.248187

[25] Kothare, M. V., Campo, P. J., Morari, M., & Nett, C. N. (1994). A unified framework for the study of anti-windup designs. *Automatica*, *30*(12), 1869-1883. https://doi.org/10.1016/0005-1098(94)90048-5